

Sub-Milli-Newton Class Miniature Microwave Ion Thruster

Yoshinori Nakayama*

National Defense Academy, Kanagawa 239-8686, Japan

and

Ikkoh Funaki[†] and Hitoshi Kuninaka[‡]

Japan Aerospace Exploration Agency, Kanagawa 229-8510, Japan

DOI: 10.2514/1.21565

A miniaturized microwave ion source with a 1.6-cm beam diameter grid system was designed and then evaluated experimentally. Based on the HAYABUSA $\mu 10$ neutralizer, we fabricated a small 18-mm-diam discharge chamber, into which 4.2 GHz microwaves were launched through an L-shaped antenna that was located in a magnetic field created by permanent magnets and iron yokes. Ion beams were emitted from the small discharge chamber when operated with a grid system whose respective hole diameters of the screen grid and acceleration grid were 0.72 and 0.43 mm, and the total number of grid holes was 211. For a beam voltage of 1500 V and a microwave input power of 10 W, the typical thruster performance was thrust of 0.34 mN, a thrust/power ratio of 16 mN/kW, propellant utilization efficiency of 68%, and a specific impulse of 3200 s. If we were able to further reduce the ion production cost (circa 3000 W/A in the current experiment), this thruster would be a candidate for main propulsion of a small satellite or precise attitude control of various sizes of satellites.

I. Introduction

FOR a main propulsion system of a small satellite or precise attitude control of various sizes of satellites, a growing demand exists these days for development of a small space propulsion system. Following demonstrations of micro-Newton and milli-Newton class thrusters such as pulsed plasma thrusters (PPT) [1] and field emission electric propulsion (FEEP) [2], a miniature ion thruster with small thrust is also proposed as an attractive candidate for a small propulsion system because the ion thruster provides high-specificity impulse and its propellant is not pollutive to the satellite surface or the environment. In general, practical ion thrusters are classified according to their plasma production type: direct current discharge (DC), radio frequency discharge (RF), and microwave discharge. Miniature DC ion thrusters have been studied and evaluated at MIT [3] and Cal-Tech. [4] Miniature RF ion thrusters were studied and evaluated at Giessen University [5] and Pennsylvania State University [6]. However, miniaturization of the microwave discharge ion thruster of the HAYABUSA asteroid explorer has been little evaluated [7].

The most attractive property of the microwave ion thruster is its electrodeless discharge, which drastically simplifies the starting-up processes that are necessary for the DC ion thruster, with its hollow cathode. The microwave ion-thruster plasma is initiated merely by switching on the microwave power supply after introducing the xenon propellant. The ion beam is then emitted by starting up a high voltage power supply. Such an easy-to-start ion thruster will be appropriate, particularly for attitude control of a spacecraft that requires a quick startup and shutdown process. Miniaturization of the microwave ion source used for $\mu 10$, however, seems difficult because the microwave is launched from a 45-mm-diam waveguide. We therefore selected a small microwave launcher design used for

the microwave neutralizer of the $\mu 10$ system. The $\mu 10$ neutralizer consists of an 18-mm-inner-diam discharge chamber, into which microwaves are introduced via a coaxial cable followed by an L-shaped 1-mm ϕ rod antenna. Such a compact discharge chamber was demonstrated as the neutralizer of the $\mu 10$ system, but it has not been operated as an ion source so far.

This paper is intended 1) to design and fabricate a miniature microwave ion thruster source (MINIT) based on the compact microwave discharge chamber design of the $\mu 10$ system with a newly developed electrostatic grid system, 2) to experimentally evaluate the ion beam emission characteristics of MINIT, and 3) to discuss the limitations and usefulness of MINIT as a small propulsion system, indicating possible improvements.

II. Thruster Design

A. Ion Production (Discharge Chamber)

The MINIT schematic is shown in Fig. 1. The design and operating conditions of MINIT are identical to those of the $\mu 10$ neutralizer [8]. No specialized tuning is applied as a miniature ion thruster. The 18-mm-diam discharge chamber comprises Sm-Co permanent magnets, cylindrical iron yokes, and an L-shaped molybdenum rod antenna. The antenna tip is located in the magnetic field formed by the magnets and the yokes. Microwave power with a frequency of 4.25 GHz is supplied to the cavity via the antenna, and the electron cyclotron resonance (ECR) region is formed between the upstream yoke tip and the downstream yoke tip. The microwave power network is matched by a single stub tuner to reduce the return microwave power. The microwave power consumed within the discharge chamber raises the temperature of the permanent magnets because of the discharge loss. Therefore, the microwave power supplied to the chamber is limited to prevent magnetic field degradation. The microwave power limitation is associated with the limitation of the propellant flow rate in the propellant utilization efficiency. A DC block is set between the tuner and the antenna for isolation of direct current. The plasma is ignited instantaneously at the start of the microwave power supply.

B. Ion Extraction (Grid System)

As described in the preceding section, the design and operating conditions of MINIT are equal to those of the $\mu 10$ neutralizer. For that reason, its grid aperture ratio is also based on that of the $\mu 10$ neutralizer. Moreover, the concern exists that the ion production cost of a miniature ion thruster is high because of the discharge chamber's

Received 6 December 2005; revision received 29 June 2006; accepted for publication 12 December 2006. Copyright © 2007 by the American Institute of Aeronautics and Astronautics, Inc. All rights reserved. Copies of this paper may be made for personal or internal use, on condition that the copier pay the \$10.00 per-copy fee to the Copyright Clearance Center, Inc., 222 Rosewood Drive, Danvers, MA 01923; include the code 0748-4658/07 \$10.00 in correspondence with the CCC.

*Associate Professor, Department of Aerospace Engineering, 1-10-20 Hashirimizu, Yokosuka; ynayama@nda.ac.jp. Member AIAA.

[†]Associate Professor, Institute of Space and Astronautical Science, 3-1-1 Yoshinodai, Sagami-hara; funaki@isas.jaxa.jp. Member AIAA.

[‡]Professor, Institute of Space and Astronautical Science, 3-1-1 Yoshinodai, Sagami-hara; kuninaka@isas.jaxa.jp. Senior Member AIAA.

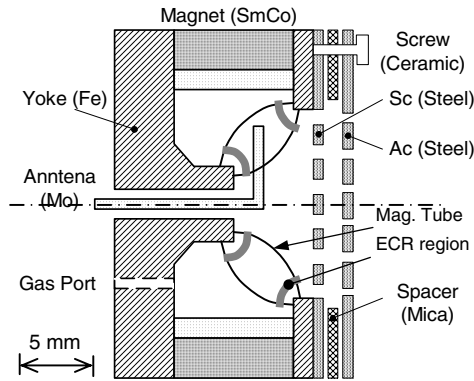


Fig. 1 Cross section of MINIT.

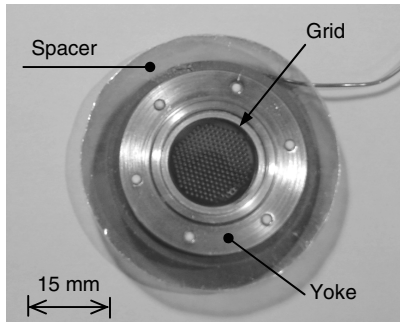


Fig. 2 MINIT grid system.

large surface-to-volume ratio. It seems that its grid system requires a concept for improved beam emission.

Ion beam emission is strongly influenced by the space charge limitation. Therefore, the optimized ion beam current per hole is determined from its geometric parameters and applied electric potential. If the plasma density is sufficiently high, it follows that the total number of grid holes dominates the total ion beam current, consequently dominating the thruster performance. As a result, the MINIT adopts a grid system with high hole-number density because of its small beam diameter, thereby preventing performance degradation arising from miniaturization.

Photographs of the MINIT grid system and a cross section of MINIT are shown, respectively, in Figs. 1 and 2. In addition, the geometric parameters of this grid system are summarized in Table 1. This geometric design was determined from numerical analyses using the OPT code [9] and the igx code [10]. The respective aperture ratios of its screen grid and acceleration grid are approximately 50 and 18%. The total hole number is 211. The hole-number density of this grid system is 120 holes/cm², which is approximately twice as high as that of conventional ion thrusters. A grid system similar to this was adopted in the miniature DC ion thruster [4]. Holes on the grids were made using a chemical etching method. The grid system comprises two stainless steel grids, a 0.25-mm-thick mica sheet, and six alumina–ceramic screws. This mica sheet and the ceramic screws are set for electrical isolation and grid suspension.

C. Thruster System

Figure 3 shows an overview of the MINIT system. A stainless steel shield case is set around the thruster to prevent interaction between the MINIT body and the neutralizer. The propellant, xenon, is supplied through a gas isolator. A 0.05-mm-diam pure tungsten filament is set downstream of the MINIT system to neutralize its ion beam.

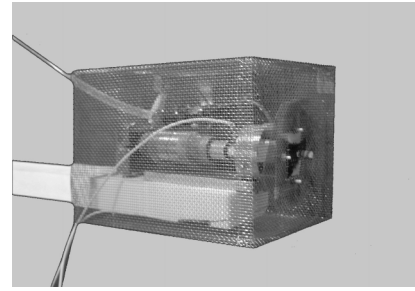


Fig. 3 MINIT system.

III. Experimental Procedure and Apparatus

A. Flow Rate Calibration

The MINIT is operated with a propellant flow rate of 0.06–0.13 sccm (6–13 $\mu\text{g/s}$, Xe), which is lower than that of conventional ion thrusters. Because a flow rate controller with sufficient accuracy in this flow rate range was unobtainable, in this study, the conventional flow rate controller with the full scale of 1.0 sccm (98 $\mu\text{g/s}$, Xe) is used with the calibration scale. The flow rate \dot{m} is calculated from the temporal change in the plenum pressure \dot{p} as

$$\dot{m}/\dot{p} = V/RT = \dot{m}_f/\dot{p}_f$$

where R is the gas constant of the propellant, and the subscript f indicates the condition of full-scale flow rate. The volume of both the gas passage and the propellant tank (V) is sufficiently large to maintain a steady flow rate control; the propellant-feed system temperature T is maintained as constant using an air conditioner. The full-scale flow rate, with its error of $\pm 1.0\%$ ($\dot{m}_f = 1.00 \pm 0.01$ sccm), had been bench-tested and guaranteed by its manufacturer. It was confirmed in our preliminary experiment that the measurement error of the \dot{p}_f was approximately $\pm 1.0\%$. Therefore, the constant V/RT is calculated from values of \dot{m}_f and \dot{p}_f using these errors. The measurement number of temporal pressure change per flow rate is greater than 70. Accordingly, the calibration scale of the flow rate is calculated statistically from measurement data using the aforementioned errors.

B. Apparatus and Facilities

A schematic of the electric circuit for this experiment is shown in Fig. 4. The screen grid is connected electrically to the discharge chamber (thruster body). It was confirmed that each part (grids, neutralizer, and shield case) is isolated electrically. This figure shows the respective current measurements of the screen grid, acceleration grid, shield case, neutralizer electron, and return; they were measured separately to confirm the precision (Kirchhoff's law). The filament neutralizer is operated to evaluate the ion emission of the grid system.

The experiment schematic is shown in Fig. 5. The distance between the ion thruster and the target wall is approximately 2.5 m. The vacuum pressure was approximately 0.3 mPa when the xenon flow rate was 0.1 sccm (10 $\mu\text{g/s}$, Xe). The thruster and its ion beam are visible from the near side and downstream through the view port.

C. Experiments

The MINIT can be operated at various conditions: the propellant flow rate of 0.06–0.13 sccm (6–13 $\mu\text{g/s}$, Xe), the microwave power is 4–18 W, the screen grid potential is 0–1500 V, and the acceleration grid potential is 0–200 V. The filament neutralizer is operated at an excessive electron condition in which the neutralizer current is higher than that of the ion beam current. The reflected microwave power and the respective currents of the screen grid, acceleration grid, shield case, and neutralizer are measured simultaneously. The ion beam

Table 1 Grid geometry

Grid	Thickness, mm	Hole diameter, mm	Pitch circle diameter, mm	Gap, mm	Aperture ratio, %	Potential, V
Screen	0.20	0.72	0.97	0.25	50	1500
Accel.	0.30	0.43			18	–200

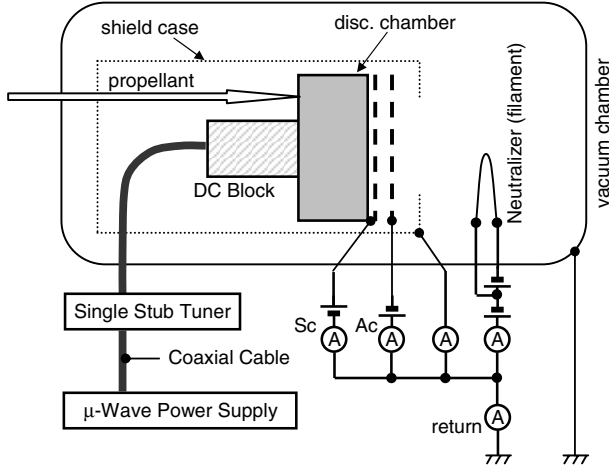


Fig. 4 Electric circuit.

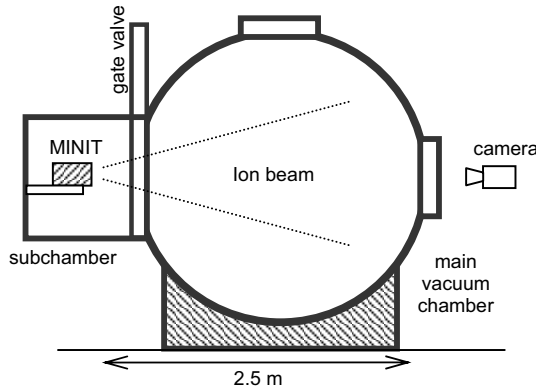


Fig. 5 Schematic of experiment.

current is calculated from the difference between the screen grid current and the sum of other currents. The thruster performance is determined using calibrated data.

IV. Results and Discussion

A. Measurement Accuracy

The calibration scale and the error rates are summarized in Table 2. As shown in that table, the net propellant flow rate is higher than the set flow rate in the operation range, and the error rate increases with a decreasing flow rate. The following data for the flow rate are calibrated with this scale. Moreover, it is confirmed that the currents, voltages, and microwave power were measured or set with negligible error.

In addition, it was verified that each grid was manufactured and located within slight error (<0.05 mm). Reproducible experimental results were obtained. Therefore, it seems that the location error of grid system was little influenced by ion beam emission.

B. Ion Beam Extraction

Figure 6 shows the grid currents against the screen grid potential when the acceleration grid potential was set at -200 V. Because the flow-in/out current of shield current was confirmed as negligible, a

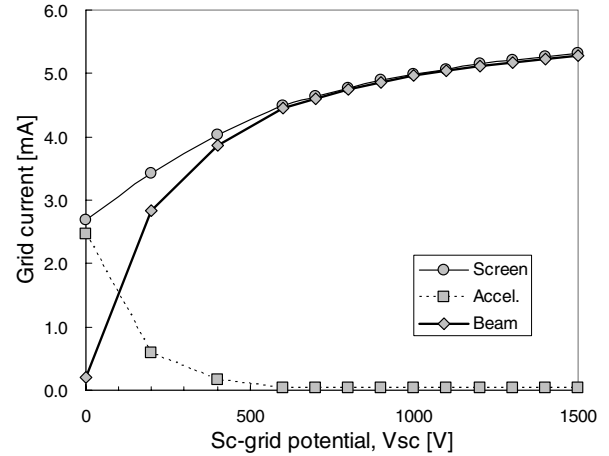


Fig. 6 Grid current (12 W, 0.108 sccm).

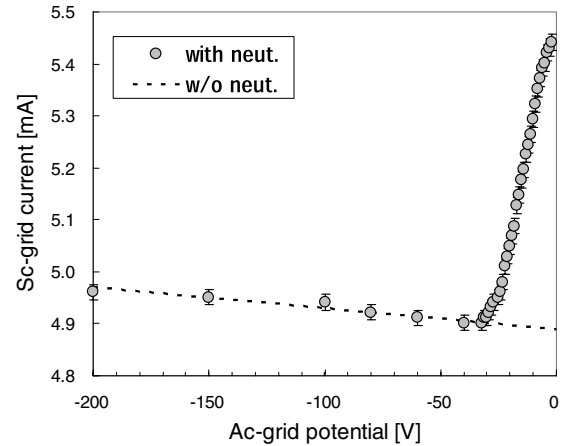


Fig. 7 Backstreaming electron (12 W, 0.108 sccm).

discharge between the discharge chamber and the neutralizer through the shield case did not occur. The figure shows that the screen grid current is almost equal to the acceleration grid current when the screen grid potential was not applied. The acceleration grid current decreases as the screen grid potential increases. Furthermore, the acceleration grid current was slight when the screen grid potential greater than 500 V. For a screen grid potential of 1500 V, the acceleration grid current is approximately 0.7% of the screen grid current. This figure indicates that the screen grid current is almost proportional to the 1.5th power of net acceleration voltage. Ion emission apparently obeys a space charge limitation.

Figure 7 shows the screen grid current against the acceleration grid potential when the screen grid potential was set at 1000 V. The broken line of this figure indicates the screen current without the neutralizer operation. The hatched circles indicate the screen current with the neutralizer operation. As shown in the figure, the screen grid current decreases as the acceleration grid potential increases without neutralizer operation. On the other hand, the screen grid current increases rapidly over -30 V acceleration grid potential with neutralizer operation. The difference between the currents clearly increases exponentially. The thermoelectrons are therefore apparently emitted from the filament neutralizer with a Maxwellian energy distribution. The electron temperature calculated from this assumption is approximately 3.7 eV. Judging from this current difference and igx analysis, the acceleration grid potential repels the neutralizer electrons in the case of -200 V acceleration grid potential.

In addition, results indicated that the electrical isolation between grids was maintained, and that the grid hole erosion was slight. This slight erosion implies that the mica grid isolator and the alumina-ceramic suspension both function well. Judging from those results, the MINIT grid system can extract an ion beam from the discharge plasma with appropriate optics.

Table 2 Calibration scale and error rate

	Error ratio	Average
Flow rate (0.08 sccm)	+8.0 to +16%	0.090 sccm
Flow rate (0.10 sccm)	+2.8 to +11%	0.108 sccm
Flow rate (0.12 sccm)	+5.9 to +11%	0.127 sccm
Currents	$<0.3\%$	—
Microwave power	-3 to $+3\%$	—

The MINIT was operated for approximately 20 h with its beam emission because the facility operation time for this study was limited. Accordingly, more investigation is necessary for proper evaluation of its beam emission.

C. Thruster Performance

Figure 8 shows the ion production cost and the propellant utilization efficiency against the calibrated propellant flow rate at input microwave power of 12 W. The ion production cost was determined by the input microwave power per unit of the ion beam current. Results indicated that the reflected microwave power was approximately 10% of the input microwave power while the MINIT was operating. This mismatch occurs because the single stub tuner cannot cancel the reflected microwave completely. Although a triple-stub tuner would be able to cancel the reflected microwave, its heavy mass would obviate its installation in a small satellite. The figure shows that the propellant flow rate at the maximum propellant utilization efficiency is different from that at the minimum ion production cost. Apparently, this difference is the reason for the high ion production cost of a few thousand W/A. Figure 9 shows the ion production cost against the propellant utilization efficiency. This evaluation shows that the maximum propellant utilization efficiency is approximately 80%.

Typical thruster performance data of the MINIT and the HAYABUSA $\mu 10$ ion thruster are presented in Table 3. The thruster performance is calculated with the input microwave power and the calibrated propellant flow rate. As shown in this table, the beam current density of MINIT is approximately 1.65 times higher than that of the $\mu 10$ ion thruster. In spite of its small discharge chamber and its low grid aperture ratio, the thrust performance of MINIT is confirmed to have propellant utilization efficiency of 68%, a specific impulse of 3200 s, and a thrust/power ratio of 16 mN/kW, which is

Table 3 Thruster performance

Performance	$\mu 10$	MINIT	Ratio
Beam diameter, cm	10.5	1.6	0.15
Net acceleration voltage, V	1500	1500	1.00
Beam current, mA	140	5.3	0.04
Beam-current density, mA/cm ²	0.4	0.66	1.65
Thrust, mN	8	0.34	0.04
Ion production cost, W/A	240	2400	10.0
Propellant utilization efficiency	87%	68%	0.78
Specific impulse, s	3200 ^a	3200	1.00
Thrust/power, mN/kW	23 ^a	16	0.70

^aWith neut. operation.

Table 4 Component list^a

Component	Mass, kg	cf.
Microwave power supply	1.5	12 W, Osc., ^b Cpl. ^c box
DC power supply	0.5	8 W, Neutralizer power
Propellant supply	1.0	FC, ^d distributor, tank
Ion engine	0.5	Thruster, neutralizer
Control system	0.5	Monitor, controller
Total	4.0	

^aHarness included in each component.

^bOsc. = oscillator

^cCpl. = coupler

^dFC = flow controller

slightly lower than that of the $\mu 10$ ion thruster. It seems that a grid system with approximately twice the hole-number density creates the high beam-current density, thereby improving the small thruster performance.

D. System Estimation

Table 4 shows the component list of MINIT as a small propulsion system. The component weight was estimated from the thruster performance ratio of MINIT and the $\mu 10$ and the actual weight of $\mu 10$ [7]. This estimation includes the electric power consumption and propellant flow rate required for neutralizer operation. The harness and chassis weights are included in the pertinent component weight. In this estimation, it is assumed that a lightweight propellant flow controller based on MEMS technology [11] is adopted in the propellant supply system.

As shown in this table, the total dry weight of the MINIT system is estimated as approximately 4 kg. Calculating from the aforementioned thruster performance, it is also estimated that MINIT requires a propellant weight of approximately 0.32 kg for 1000 Ns impulse generation. Although the PPT is installed to NASA EO-1, which has a total wet weight of 4.95 kg, it can generate a total impulse of 460 Ns [1]. The MINIT system, with equal weight, can generate a total impulse of approximately 3000 Ns. This propulsion system, with a total impulse of 3000 Ns, can keep a 50 cm cubic satellite in a 400-km-altitude orbit for over seven years.

E. Future Work

The MINIT thruster efficiency was only 2.7% because of its high ion production cost. The ion production cost of the MINIT is over three times as high as that of the DC miniature ion thruster [4]. That high cost implies that the plasma production of MINIT is inefficient. The main reason might be that the MINIT design and operating conditions are identical to those of the $\mu 10$ neutralizer. That is, no specialized tuning was applied, as with the miniature ion thruster. The modifications and matching of its plasma production (power, frequency, and magnetic field) and its grid system (aperture ratio and hole number) are necessary for performance improvement.

In addition, the present study has neglected discussion of another problem: the difficulty of development and fabrication of the MINIT system's miniature neutralizer. The electron production cost of the miniature neutralizer is higher than that of a conventional neutralizer

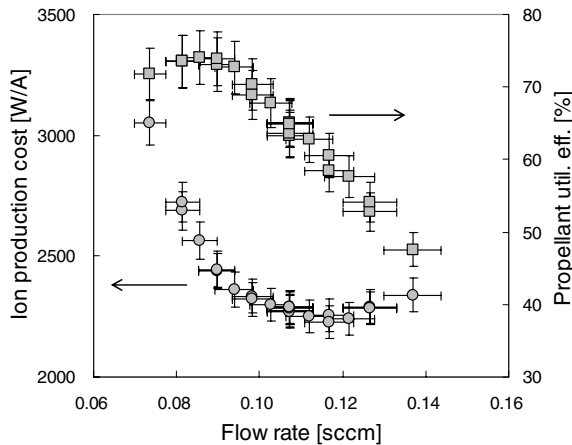


Fig. 8 Effect on flow rate (12 W, 1500/ – 200 V).

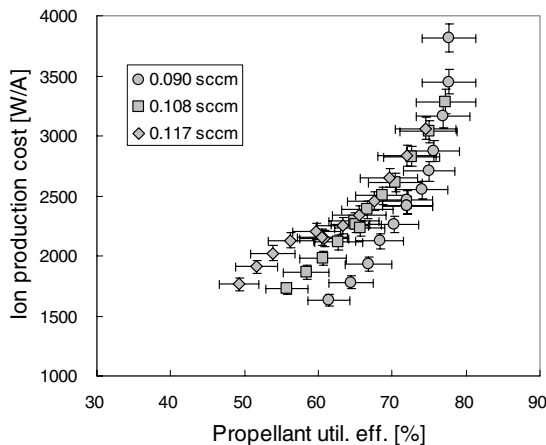


Fig. 9 Plasma production (12 W, 1500/ – 200 V).

because of its small discharge chamber. Its high cost degrades the thruster performance. This problem is unavoidable for system establishment, in common with other miniature ion thrusters. In this paper, a field emission array (FEA) is proposed for the neutralizer. Kitamura et al. [12] confirmed that their developed FEA offers high electron current density and durability. The FEA can generate sufficient electron current required for the neutralization without plasma interaction between the ion beam and the neutralizer. Therefore, it seems that the FEA, which requires no working gas, is an attractive miniature neutralizer.

Development of miniature neutralizers and more detailed investigations are necessary before the actual use in space. Moreover, the system estimation compared to other miniature ion thrusters remains to be discussed because of the lack of thruster information. However, the present MINIT system has properties for installation in small satellites in spite of its inefficient plasma production. It seems reasonable to presume that the improved MINIT system can be a candidate for small propulsion systems, similar to PPT and FEEP.

V. Conclusions

Through the fabrication and experimental investigation of miniature ion thruster with 1.6-cm beam diameter based on the neutralizer of the HAYABUSA $\mu 10$ microwave ion thruster (MINIT), the following results were obtained:

- 1) A compact ECR discharge chamber with power introduction via coaxial cable can be operated as an ion source.
- 2) A grid system with approximately twice the hole-number density improves the thruster performance of the miniature ion thruster.
- 3) Typical thruster performance of MINIT includes thrust of 0.34 mN, a thrust/power ratio of 16 mN/kW, propellant utilization efficiency of 68%, and a specific impulse of 3200 s.
- 4) The MINIT system, with a 5.0 kg wet weight, can generate total impulse of approximately 3000 Ns.
- 5) Plasma production improvement and miniature neutralizer development are required for actual use in space.
- 6) The improved MINIT system will be a candidate to meet small propulsion requirements.

References

- [1] Pencil, E., Kamhawi, H., and Arrington, L., "Overview of NASA's Pulsed Plasma Thruster Development Program," AIAA Paper 2004-3455, 2004.
- [2] Marcuccio, S., "The Design of Micronewton FEEP Thrusters for Disturbance Reduction Systems," IEPC Paper 03-241, 2003.
- [3] Yashko, G. J., Griffin, G. B., and Hastings, D. E., "Design Considerations for Ion Microthrusters," IEPC Paper 97-072, 1997.
- [4] Wirz, R., Gale, M., Mueller, J., and Marrese, C., "Miniature Ion Thrusters for Precision Formation Flying," AIAA Paper 2004-4115, 2004.
- [5] Felli, D., Loeb, H. W., Scharfner, K. H., Weis, S., Kirmse, D., Meyer, B. K., Kilinger, R., Mueller, H., and Di Cara, D. M., "Performance Mapping of New μ N-RITs at Giessen," IEPC Paper 2005-252, 2005.
- [6] Mistoco, V., Trudel, T., Bilen, S., and Micci, M., "Vacuum Testing of the Miniature Radio-Frequency Ion Thruster," IEPC Paper 2005-265, 2005.
- [7] Kuninaka, H., Nishiyama, K., Shimizu, Y., Toki, K., Kawaguchi, J., and Uesugi, K., "Initial Operation of Microwave Discharge Ion Engines Onboard 'HAYABUSA' Asteroid Explorer," *Journal of the Japan Society for Aeronautical and Space Sciences*, Vol. 52, No. 602, 2004, pp. 129–134.
- [8] Funaki, I., Kuninaka, H., and Toki, K., "Plasma Characterization of a 10-cm Diameter Microwave Discharge Ion Thruster," *Journal of Propulsion and Power*, Vol. 20, No. 4, 2004, pp. 718–727.
- [9] Arakawa, Y., and Ishihara, K., "A Numerical Code for Cusped Ion Thruster," IEPC Paper 91-118, 1991.
- [10] Nakayama, Y., and Wilbur, P. J., "Numerical Simulation of Ion Beam Optics for Multiple-Grid Systems," *Journal of Propulsion and Power*, Vol. 19, No. 4, 2003, pp. 607–613.
- [11] Cardin, J., and Otsap, B., "A Digital Xenon Flow Controller Based on ChEMS Technology," IEPC Paper 99-064, 1999.
- [12] Kitamura, S., Nishida, S., Iseki, Y., and Okawa, Y., "Preliminary Study on Field Emitter Array Cathodes for Electro-dynamic Tether Propulsion," *Proceedings of the Asian Joint Conference on Propulsion and Power 2004*, JSASS0, Tokyo, 2004, pp. 1–6.

A. Gallimore
Associate Editor